

Experimental Study of a Toroidal Plasma under the Conditions for Adiabatic Budker-Buneman Instability

A. Hirose, J. D. Paulson, H. M. Skarsgard, and S. Wolfe

Department of Physics, University of Saskatchewan, Saskatoon, Saskatchewan S7N 0W0, Canada

(Received 13 May 1983)

Conditions suitable for the adiabatic electron-ion two-stream instability have been created in a toroidal plasma. Observed anomalous resistivity, turbulent heating rates, and ion plasma oscillations are in favorable agreement with the recent theoretical predictions.

PACS numbers: 52.35.Py, 52.35.Fp, 52.50.Gj

The Budker-Buneman instability^{1,2} was predicted some twenty years ago and is considered to play important roles in turbulent heating³ and space plasma.⁴ The instability requires an electron drift velocity far exceeding the thermal velocity. However, this condition cannot be easily realized in laboratory plasmas. Usually strong electric fields higher than the Dreicer critical field are applied to accelerate electrons but this only results in partial free acceleration accompanied by efficient turbulent heating of electrons, and consequently the drift velocity never exceeds the thermal velocity by a factor of more than 2. This phenomenon has been confirmed both in computer simulations⁵ and in a toroidal experiment.⁶ An instability related to the Budker-Buneman instability has been observed in a plasma having electrodes.⁷ In this case, however, electrons are continuously replenished, and one of the most important aspects of the Budker-Buneman instability, namely turbulent heating of electrons and ions, cannot be studied in such a system. The instability and its several nonlinear aspects predicted by Buneman can only be studied in a plasma well confined, and having no external electric field. The latter requirement is necessary because the numerical simulation done by Buneman was on a relaxation problem without any external fields. Therefore, conventional turbulent-heating experiments having pulse length much longer than the characteristic growth time of the instability are not really suitable for studying the instability in a clear-cut manner.

The present study has been motivated not only by creating experimental conditions suitable for the instability, but also by the recent advancement in theoretical understanding of the instability.⁸ Major theoretical findings are these: (a) The so-called Buneman frequency $\omega_B = \frac{1}{2}(m/2M)^{1/3} \times \omega_{pe}$ (m/M is the electron/ion mass ratio, ω_{pe} the electron plasma frequency) is not an observable quantity because of strong nonlinear frequen-

cy modulation. (b) In addition to well expected electron heating, ions too can gain a kinetic energy in excess of 10% of the initial electron drift energy. (c) The anomalous collision frequency scales as $(m/M)^{0.61}$ rather than $(m/M)^{1/3}$.⁹ All of these predictions are in favorable agreement with experimental observations as will be shown.

The plasma betatron¹⁰ used in the experiment has a major radius of 19 cm, a minor radius of 3 cm, toroidal magnetic fields up to 4 kG and initial electron densities controllable in the range 4×10^{10} to 1×10^{11} cm⁻³. An argon plasma is prepared by an rf discharge. The increase in the electron density during the interval of interest (300 nsec) is at most 20%, due to additional ionization of neutrals. The filling pressure is $(0.3-0.5) \times 10^{-3}$ Torr.¹¹ A betatron-type poloidal magnetic field configuration is produced by four windings, which are energized by a 7.5-nF, 30-kV capacitor bank. The primary current is cross-barred at the quarter period, approximately 130 nsec. The electric field pulse thus created has a half-width of about 100 nsec, and the peak vacuum intensity of up to 50 V/cm.¹² Such a short pulse will accelerate electrons freely at least initially. Experimentally, it has been found that electrons are freely accelerated for the first 100 nsec. Diagnostics include Rogowsky coil, Langmuir probes, 2-cm microwave interferometer, electron-energy analyzer, and optical spectrometer for ion-energy measurements.

Figure 1 shows observed loop voltage (before inductance correction) and total plasma current (top photograph). The lower diagram shows the electric field (after induction correction), the electron drift velocity calculated from measured total current and electron density (skin effect is negligible), and the electron drift velocity expected from free acceleration, for the case of initial electron density of 5×10^{10} cm⁻³. The free acceleration lasts for about 100 nsec, followed by departure from free acceleration and a rapid

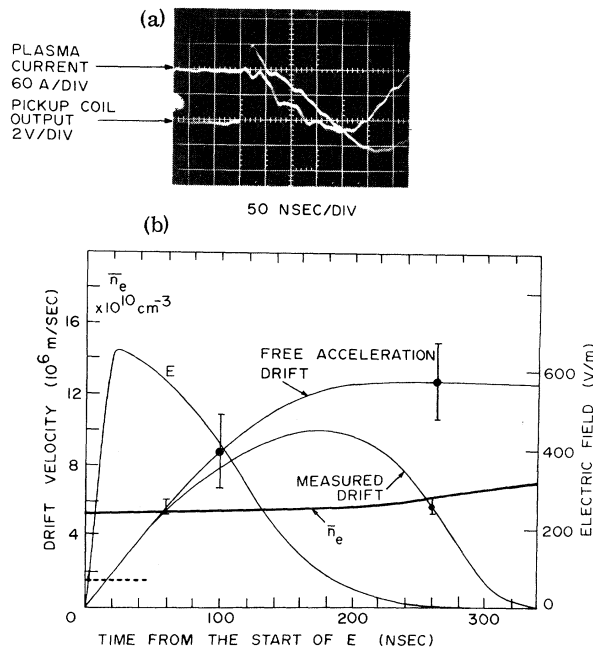


FIG. 1. (a) Loop voltage and plasma current. \bar{n}_e (average initial electron density) = $5 \times 10^{10} \text{ cm}^{-3}$, $B_T = 1.6 \text{ kG}$. (b) Deduced electric field, corresponding free-acceleration drift velocity, measured (through I_D and \bar{n}_e) drift velocity, initial thermal velocity (dashed line), and $\bar{n}_e(t)$.

current collapse. The initial electron thermal velocity corresponding to the electron temperature measured by double Langmuir probe during rf discharge is indicated by the dashed line in the figure. It can be seen that the electron drift velocity exceeds the initial thermal velocity by a factor of at least 7 which should be sufficient for the Budker-Buneman instability to be operative.¹³ Also, after the end of free acceleration, the plasma is essentially free of the electric field thus making itself adiabatic (isolated from external energy source).

The electron-energy analyzer¹⁴ can only sample the energy perpendicular to the magnetic field. Figure 2 shows the energy distribution observed at 320 nsec under the same condition as Fig. 1. As previously observed in the same device,¹⁰ the electron distribution is remarkably Maxwellian. Furthermore, the measured thermal energy agrees well with the energy input provided an isotropic Maxwellian is assumed. [The problem of electron heating perpendicular to a strong (ω_{ce} , electron cyclotron frequency, $> \omega_{pe}$, electron plasma frequency) magnetic field has recently been resolved¹⁵ for the case of current-driven

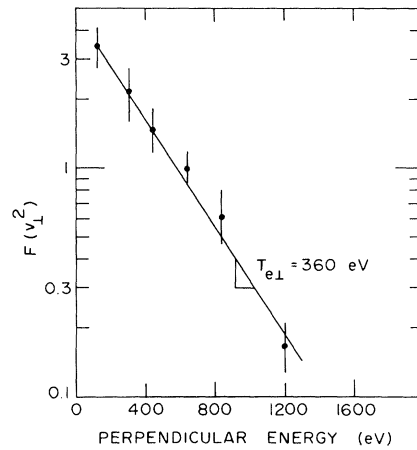


FIG. 2. Example of measured electron perpendicular energy distribution. Same conditions as Fig. 1, $t = 0.32 \mu\text{sec}$.

ion acoustic instability. It has been demonstrated that cross-field heating is as effective as parallel heating, and temperature equilibration is extremely rapid governed by the anomalous collision frequency.]

Figure 3 shows the total energy input, the electron drift energy, expected thermal energy density, and the collision frequency, calculated from $\nu = (eE - m \dot{V}_D)/mV_D$, where V_D is the drift velocity and \dot{V}_D its time derivative. Complete thermalization of the initial electron drift energy can be clearly seen. Also, the agreement between the expected and measured thermal energy contents ensures that the plasma is loss free at least during the first 300 nsec. The classical collision frequency dominated by electron-neutral collisions is of the order of $5 \times 10^6/\text{sec}$, which is too small to explain the observed rapid and complete thermalization. We believe that this anomalous rapid thermalization is due to the onset of the Budker-Buenman instability.

Unfortunately, identification of the instability cannot be done through frequency spectrum of fluctuations since as mentioned before the linear Buneman frequency corresponding to the fastest growing mode is expected to be unobservable because of severe nonlinear frequency modulation.⁸ During one period of oscillation ($2\pi/\omega_B$) the instability will have e -folded by a factor of 5.4×10^4 [$= \exp(2\pi\sqrt{3})$] in field and 3×10^9 in energy. Since the thermal level of fluctuations is of the order of 5×10^{-8} and energy deposited in the plasma is only 40 times the initial thermal energy, it is

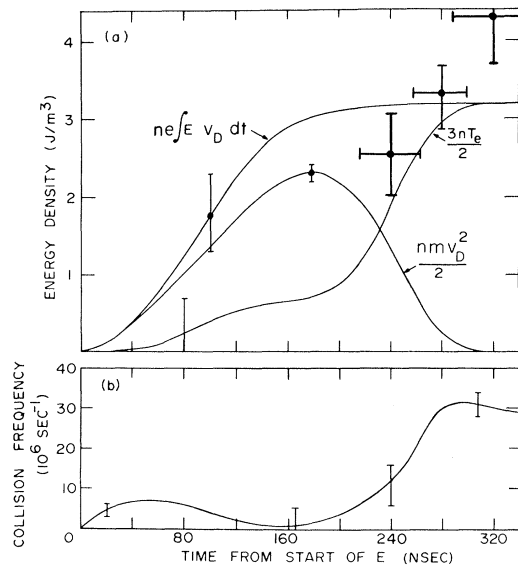


FIG. 3. (a) Energy input, electron drift energy, and expected thermal energy. Dots indicate measured (through T_e and \bar{n}_e) electron thermal energy density. Same conditions as Fig. 1. (b) Time evolution of the electron collision frequency.

expected that nonlinearity and saturation set in before one Buneman oscillation is completed. (Note that the instability saturates when the fluctuation level becomes of the order of $0.1 \times$ electron drift energy.⁸) However, in the aftermath of the instability, or after thermalization is completed, strong ion oscillation is expected to develop.⁸ The oscillation frequency is close to the ion plasma frequency ω_{pi} , and of incomplete standing-wave nature.

Langmuir probes were used to detect potential fluctuations. An example is shown in Fig. 4 (inset). Note that during the first 200 nsec, no oscillations are seen. Oscillations start at about 200 nsec, and persist afterward. The frequency spectrum obtained by averaging five oscillograms indicates relatively coherent oscillations with a frequency close to the ion plasma frequency. f_{pi}^0 in the figure indicates the ion plasma frequency corresponding to the initial peak plasma density, which is approximately $2\bar{n}_e$, and f_B indicates the Buneman frequency. The frequency has been observed to exhibit the expected $\sqrt{\bar{n}_e}$ dependence.

With use of two Langmuir probes, attempts have been made to detect the propagation nature of the oscillations at the ion plasma frequency. No continuous phase shifts with the probe separation have been detected in any direction (parallel or perpendicular to the toroidal magnetic field).

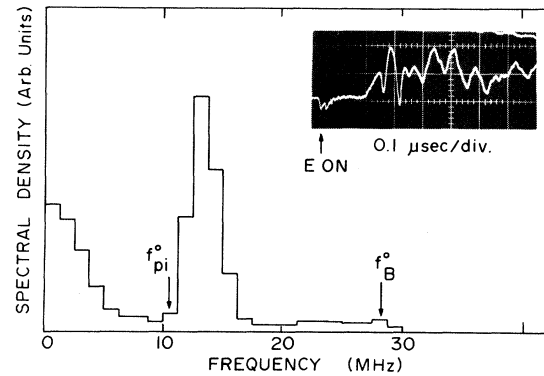


FIG. 4. Example of measured fluctuation (inset) and frequency spectrum. Probe location 2 cm from the outer wall. f_{pi}^0 and f_B^0 are the ion plasma and Buneman frequency corresponding to the initial peak electron density.

This seems to indicate that the fluctuations are largely standing-wave nature, although definite conclusions cannot be drawn at the present stage.

As shown in Fig. 1, the electron drift velocity exceeds the initial thermal velocity as early as 20 nsec, and the condition for the hydrodynamic Budker-Buneman instability ($V_D \gtrsim 6v_{th}$) becomes satisfied at about 100 nsec. One then expects that oscillations (exponentially growing) at f_B are to be observed starting at about 100 nsec. However, it should be recalled that the frequency f_B is that of the fastest growing mode characterized by the resonance condition, $kV_D = \omega_{pe}$. Therefore, if the drift velocity changes rapidly, a particular mode with a definite wavelength can hardly grow. Only when the drift velocity acquires a (quasi) steady value will the instability set in to destroy the current. The effective onset time of the instability may then be estimated as 160–200 nsec, before which no oscillations at f_B are expected.

The ion energy distribution both parallel and perpendicular to the magnetic field has been measured spectroscopically by monitoring the 4806-Å Ar II line. Because of the low densities employed, observation was possible only at 0.5 μ sec or later, well after the collapse of the electron drift. The observed distribution is strongly anisotropic, accompanied by preferential ion heating along the toroidal direction with an effective temperature of 50 eV under the same conditions as Fig. 1. The observed parallel distribution is, however, hardly Maxwellian, indicating a relatively long relaxation time for ions.

Finally, we note that the observed maximum

collision frequency $3 \times 10^7/\text{sec}$ [Fig. 3(b)] compares favorably with the theoretical value⁸ $(m/M)^{0.61} \omega_{pe} = 1.4 \times 10^7/\text{sec}$.

In conclusion, we have created in a toroidal plasma conditions suitable for studying the adiabatic Budker-Buneman instability. Complete thermalization of electrons is observed followed by the appearance of relatively coherent ion oscillations at frequencies close to the ion plasma frequency. The results are in general agreement with the recent theoretical predictions.

Helpful discussions with Dr. O. Ishihara, Professor I. Alexeff, and Professor O. Buneman are gratefully acknowledged. We also thank Mr. J. Ratzlaff and Mr. A. Witmans for technical assistance. Research was sponsored by the Natural Sciences and Engineering Research Council of Canada.

¹G. I. Budker, Dokl. Akad. Nauk SSSR 107, 807 (1956) [Sov. Phys. Dokl. 1, 218 (1957)].

²O. Buneman, Phys. Rev. 115, 503 (1959).

³See, for example, E. D. Voklov, N. F. Perepelkin, V. A. Suprunenko, and E. A. Sukhomlin, *Kollektivnie Yavlenia v Tokonesuchei Plazmy* (Collective Phenomena in Current Carrying Plasma) (Nauk. Dumka, Kiev, 1979) (in Russian). Some 300 references are cited.

⁴J. M. Kindel, C. Barnes, and D. W. Forslund, in *Physics of Auroral Arc Formation*, edited by S. I. Akasofu and J. R. Kan, Geophysical Monograph Series Vol. 25 (American Geophysical Union, Washington,

D.C., 1981), p. 303.

⁵J. P. Boris, J. M. Dawson, J. H. Orens, and K. V. Roberts, Phys. Rev. Lett. 25, 706 (1970).

⁶A. Hirose and H. M. Skarsgard, Phys. Rev. Lett. 36, 252 (1976).

⁷S. Iizuka, K. Saeki, N. Sato, and Y. Hatta, Phys. Rev. Lett. 43, 1404 (1979).

⁸O. Ishihara, A. Hirose, and A. B. Langdon, Phys. Rev. Lett. 44, 1404 (1980), and Phys. Fluids 24, 452 (1981), 25, 610 (1982).

⁹S. M. Hamburger and J. Jancarik, Phys. Fluids 15, 825 (1972).

¹⁰A. Hirose and H. M. Skarsgard, Plasma Sci. 5, 66 (1977).

¹¹Depending on the duration of rf discharge, the actual neutral density can be substantially smaller than that corresponding to the filling pressure as a result of "burnout."

¹²The electric field is measured by a one-turn pickup coil having a diameter of 11.4 cm and located on a plane 17 cm below the midplane. Mutual inductances among the loop, the four poloidal windings, and the plasma ring, the plasma self-inductance, and the attenuation factor in the circuit yield the net electric field (the field responsible for electron acceleration and heating) in the absence of skin effect,

$$E = 197V_0 - 3.24 \times 10^{-7} dI_p/dt \text{ (V/m)}$$

where V_0 (in volts) is the output voltage (shown in Fig. 1, top) and I_p (in amperes) is the plasma current. Details can be found in A. R. Strilchuk, Ph.D. thesis, University of Saskatchewan, 1971 (unpublished).

¹³J. D. Jackson, J. Nucl. Energy, Pt. C 1, 171 (1960).

¹⁴D. J. Loughran, L. Schott, and H. M. Skarsgard, Can. J. Phys. 45, 3055 (1967).

¹⁵O. Ishihara and A. Hirose, Phys. Rev. Lett. 50, 1783 (1983).

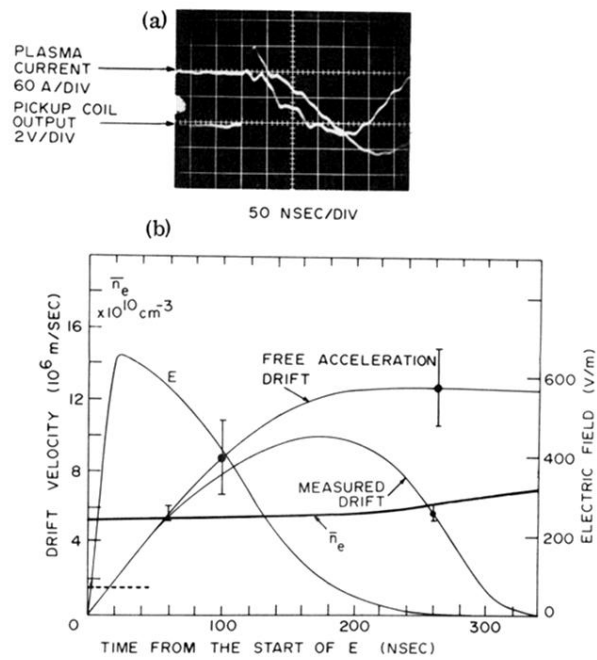


FIG. 1. (a) Loop voltage and plasma current. \bar{n}_e (average initial electron density) = $5 \times 10^{10} \text{ cm}^{-3}$, $B_T = 1.6 \text{ kG}$. (b) Deduced electric field, corresponding free-acceleration drift velocity, measured (through I_p and \bar{n}_e) drift velocity, initial thermal velocity (dashed line), and $\bar{n}_e(t)$.

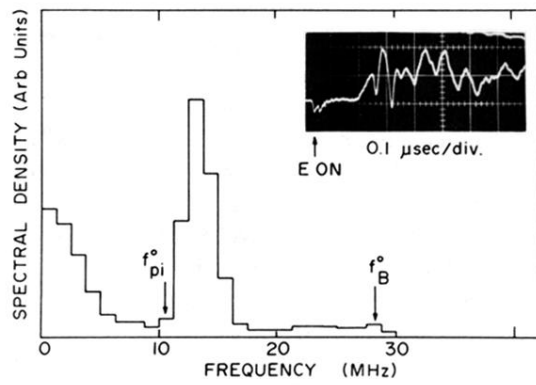


FIG. 4. Example of measured fluctuation (inset) and frequency spectrum. Probe location 2 cm from the outer wall. f_{pi}^0 and f_B^0 are the ion plasma and Buneman frequency corresponding to the *initial* peak electron density.